Order-Disorder Phase Transition in a Chaotic System

Rinto Anugraha,[1,*] Koyo Tamura,[1] Yoshiki Hidaka,[1] Noriko Oikawa,[1] and Shoichi Kai[1,2]

[1]*Department of Applied Quantum Physics and Nuclear Engineering, Graduate School of Engineering, Kyushu University, Fukuoka 819-0395, Japan*

[2]*Department of Systems Life Sciences, Graduate School of Systems Life Sciences, Kyushu University, Fukuoka 812-8581, Japan*

(Received 3 September 2007; published 24 April 2008)

For soft-mode turbulence, which is essentially the spatiotemporal chaos caused by the nonlinear interaction between convective modes and Goldstone modes in electroconvection of homeotropic nematics, a type of order-disorder phase transition was revealed, in which a new order parameter was introduced as pattern ordering. We calculated the spatial correlation function and the anisotropy of the convective patterns as a 2D *XY* system because the convective wave vector could freely rotate in the homeotropic system. We found the hidden order in the chaotic patterns observed beyond the Lifshitz frequency f_L, and a transition from a disordered to a hidden ordered state occurred at the f_L with the increase of the frequency of the applied voltages.

DOI: 10.1103/PhysRevLett.100.164503 PACS numbers: 47.52.+j, 47.27.Cn, 61.30.Gd, 64.60.Cn

Phase transitions have been researched extensively in several branches of physics [1]. The most well-known example is a transition from the ferromagnetic phase to the paramagnetic phase by changing temperature T, being a category of order-disorder phase transition due to spontaneous symmetry breaking, where thermal fluctuations play an important role [2]. Therefore, in order to understand such transitions more deeply, the statistical properties and dynamics of fluctuations must be clarified. For nonequilibrium open systems, it is thought that nonthermal fluctuations such as chaos play the similar role to thermal fluctuations. In the present study, we examine spatiotemporal chaos (STC) in a system with a specific symmetry, which induces Goldstone modes. Our STC is called soft-mode turbulence (SMT) and is observed in electroconvection systems of nematic liquid crystals (NLCs) [3].

There are two different alignments for NLCs, namely, the planar alignment and the homeotropic alignment. In the planar (homeotropic) alignment, the director $\mathbf{n}$ of an NLC is parallel (perpendicular) to the x-y plane. In the planar system, a convective stripe pattern appears when the ac voltage V applied to a thin layer of the planar NLC exceeds a threshold V_c, and a homogeneous wave vector $\mathbf{q}$ of the stripe pattern appears. On the other hand, in the homeotropic system, the first transition called the Fréedericksz transition occurs at $V = V_F$, below V_c. The director tilts with respect to the z axis by the transition, and its projection on the x-y plane is called the $\mathbf{C}(\mathbf{r})$-director, where $\mathbf{r} = (x, y)$. Since the transition spontaneously breaks the continuous rotational symmetry on the x-y plane, the rotation of $\mathbf{C}(\mathbf{r})$ behaves as Goldstone modes [4–6]. Electroconvection also appears in the homeotropic system in the same manner as the tilted director appears in the planar system. The nonlinear interaction between the resulting convective modes $\mathbf{q}$ and the Goldstone modes $\mathbf{C}$ leads to the SMT [3]. The local wave vector $\mathbf{q}(\mathbf{r})$ can be defined in the SMT (see Fig. 1 in [7]). There are two types of stripe patterns in the electroconvection of the NLC in the planar system, namely, normal rolls (NR) and oblique rolls (OR) [8]. With respect to the initial director, the homogeneous wave vector of convection is parallel and oblique in the NR and the OR, respectively. Similar to the NR and the OR in the planar case, the local convective wave vector $\mathbf{q}(\mathbf{r})$ in the SMT is either parallel to the local director $\mathbf{C}(\mathbf{r})$ in the NR or oblique in the OR in the homeotropic system [4]. In the phase diagram of the applied voltage—ac frequency ($V - f$), there exists the Lifshitz point as a codimension two

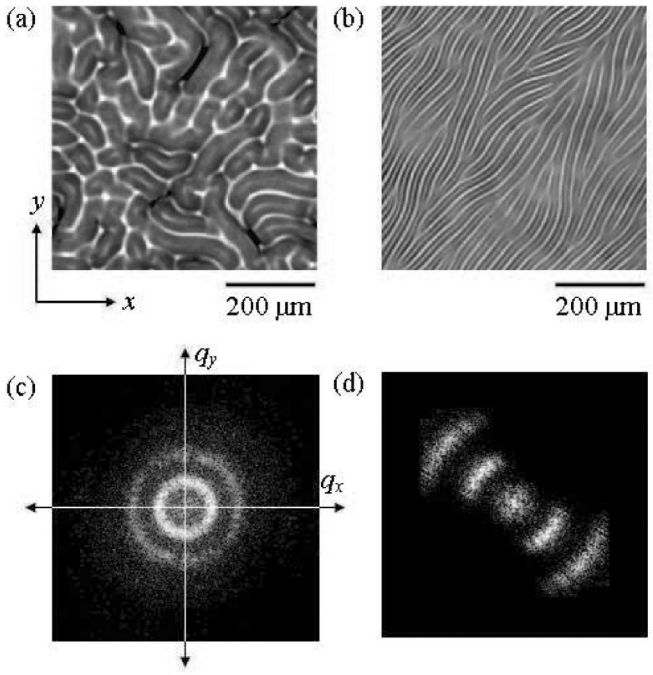

FIG. 1. Images of the SMT ($\varepsilon = 0.1$) in cell II in (a) the OR regime ($f = 200$ Hz) and (b) the NR regime ($f = 1000$ Hz). The spectra, which are calculated from (a) and (b), are shown in (c) and (d), respectively.

point. The frequency at this point is called the Lifshitz frequency f_L, which separates the OR ($f < f_L$) and the NR regimes ($f > f_L$) [9,10]. Although the SMT appears in both regimes of NR and OR [11], the interaction between the convective and Goldstone modes are different [12–14]. The properties of fluctuations in the SMT therefore depend on the details of the interaction. We investigated the spatial fluctuations in the SMT using the spatial correlation function of $\mathbf{q}(\mathbf{r})$. In the present study, we report experimental results on the order-disorder phase transition of chaotic patterns in a nonequilibrium open system characterized by a newly defined order parameter, called pattern ordering.

Because of the existence of the Goldstone modes in the SMT, we are interested in comparison with a well-known 2D XY model, which also possesses the Goldstone modes, and as a consequence no ordered state in the model is realized [15]. Nevertheless, the Kosterlitz-Thouless (KT) phase transition was discovered in the conventional model [16]. With respect to the dimension of systems as well as degree of freedom of variables, both the SMT and the conventional 2D XY model are similar, although the present study considers chaos in a nonequilibrium open system. Therefore, research by analogy with the 2D XY model may be useful to understand the statistical properties of the SMT.

The experimental setup and the sample cell using a nematic liquid crystal p-methoxy-benziliden-p'-n-buthylannyline (MBBA) were similar to those in the previous paper [7]. In the present experiment, we used two sample cells, cell I ($d = 50 \pm 2$ μm) and cell II ($d = 51 \pm 2$ μm). Here, d is the cell thickness. Although the properties of both cells were slightly different, the results obtained from both were qualitatively the same. The electrodes in both cells are circular and have the same diameter of 13.0 mm. The experimental temperature was stabilized to be 30.00 ± 0.05 °C. The dielectric constant $\epsilon_\parallel$ and the electric conductivity $\sigma_\parallel$ of the material in cell I (II) were 3.53 ± 0.05 (3.30 ± 0.10) and $3.3 \pm 0.1 \times 10^{-7}$ $\Omega^{-1}\,\mathrm{m}^{-1}$ ($2.7 \pm 0.1 \times 10^{-7}$ $\Omega^{-1}\,\mathrm{m}^{-1}$), respectively. An alternating voltage $V_{\mathrm{ac}}(t) = \sqrt{2}V\cos(2\pi f t)$ was applied perpendicular to the sample. We define a normalized control parameter $\varepsilon \equiv (V/V_c)^2 - 1$. The pattern images in the x-y plane were captured using a CCD camera (QImaging Retiga 2000R-Sy) mounted on a microscope and software (QCAPTURE PRO v.5). The size of the captured images was 1.14 mm × 1.14 mm (1000 pixel × 1000 pixel). The image analysis was performed by custom software.

By observing patterns with the change of frequency at fixed $\varepsilon = 0.05$, we obtained f_L for cell I and cell II as 380 Hz and 250 Hz, respectively [17]. Figures 1(a) and 1(b) show typical images in the OR regime observed below f_L and the NR regime beyond f_L, respectively. We performed the following procedures to obtain the images. First, the ac voltage was increased by the Fréedericksz transition state, and we waited for a sufficient time (≈ 30 min) to remove the inhomogeneous director orientation before a convection state. Then, we set the desired positive control parameter ε by jumping to the voltage above a convective threshold, and captured the images after waiting for 10 min in order to avoid the transient state. A spectrum shown in Fig. 1(c) corresponding to Fig. 1(a) indicates an isotropic property of the pattern in the OR regime. On the other hand, the anisotropic feature of the pattern shown in Fig. 1(b) can be recognized both in the real image and in the spectrum. Although we can qualitatively distinguish the SMT patterns in the OR and the NR regimes taking their spectra, we need more quantitative information for further discussion.

Now, let us introduce the spatial correlation function $S(r)$ defined as

$$S(r) = \langle \cos 2[\phi(\mathbf{r} + \mathbf{r}_0) - \phi(\mathbf{r}_0)] \rangle_{\mathbf{r}_0} \qquad (1)$$

where $r = |\mathbf{r}|$. Here, $\phi(\mathbf{r})$ is the azimuthal angle of the local wave vector $\mathbf{q}(\mathbf{r}) = (q_0 \cos\phi(\mathbf{r}), q_0 \sin\phi(\mathbf{r}))$, where q_0 is assumed to be constant and $-\frac{\pi}{2} < \phi(\mathbf{r}) \leq \frac{\pi}{2}$. The angle $\phi(\mathbf{r})$ is obtained by the local spectrum method [7,18]. We show the correlation function $S(r)$ for patterns in the OR and NR regimes by changing f (fixed ε) in Fig. 2. We fitted the data by the least mean square method to the function $S(r) = S_\infty + (1 - S_\infty)\exp(-r/\xi)$ [19]. S_∞ for the OR regime is equal to zero, and S_∞ for the NR regime is finite. This can be interpreted as the absence of macroscopic order in the SMT patterns in the OR regime, but the order exists in the NR regime.

However, the local spectrum method needs one arbitrary parameter, i.e., the clipped image size (expressed as m in

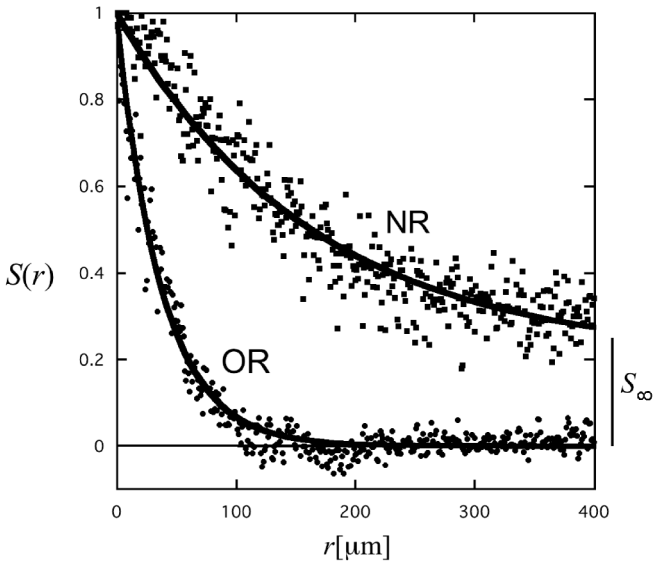

FIG. 2. Spatial correlation $S(r)$ for the OR (circle) and NR (rectangular) regimes for a fixed $\varepsilon = 0.05$, $f = 300$ Hz (OR), $f = 500$ Hz (NR). These data were taken from cell I. The thick lines are determined by the fitting (see text).

Ref. [7]). To avoid the obscurity in $\phi(\mathbf{r})$ due to that, a new order parameter obtained directly from 2D spectra is introduced. Here, since the $\mathbf{q}(\mathbf{r})$ field can freely rotate and its norm is almost constant, it has the same degree of freedom as that in the 2D XY model. Therefore, we use the formula of magnetization in the 2D XY model to the present system. A scalar magnetization in a discrete 2D XY model is defined as $M = (1/N)\Sigma_{i=1}^{N} \cos(\phi_i - \bar{\phi})$, where $\bar{\phi} = \tan^{-1}(\Sigma_i \sin\phi_i / \Sigma_i \cos\phi_i)$ is averaged ϕ_i and N is the number of cites in the system [20]. The formula can be applied to our pattern ordering M_p, which can show the order of $\mathbf{q}(\mathbf{r})$. Since the $\mathbf{q}(\mathbf{r})$ vector has a symmetry with respect to ϕ-rotation ($\mathbf{q} \rightarrow -\mathbf{q}$ symmetry), the pattern ordering should be written as

$$M_p = \langle \cos 2(\phi - \langle\phi\rangle)\rangle = \frac{\int_{-\pi/2}^{\pi/2} B(\phi)\cos 2(\phi - \langle\phi\rangle) d\phi}{\int_{-\pi/2}^{\pi/2} B(\phi) d\phi}, \tag{2}$$

where $\langle\phi\rangle$ and $B(\phi)$ are the spatial average and the distribution function of $\phi(\mathbf{r})$, respectively [18]. Using the fast Fourier transform (FFT), the amplitude spectrum $J(\mathbf{q}) = J(q, \phi)$ can be obtained from the intensity of the SMT pattern $I(x, y)$. $B(\phi)$ can be obtained as $J(q_0, \phi)$ when the magnitude of $\mathbf{q}$ is assumed to be a constant q_0. A completely isotropic pattern corresponding to $B(\phi) =$ constant gives $M_p = 0$, and a completely ordered pattern gives $M_p = 1$ because $B(\phi) = B_0 \delta(\phi - \phi_0)$, where B_0 is constant and ϕ_0 lay along the preferred axis. Therefore, M_p is bounded in $0 \leq M_p \leq 1$. Actually, since the spectrum is broad in the $\mathbf{q}$-direction [see Figs. 1(c) and 1(d)], we used $B(\phi) = \int_{q_0-\Delta q}^{q_0+\Delta q} J(q, \phi) dq$ instead of $B(\phi) = J(q_0, \phi)$, where $2\Delta q$ indicates the broadness of the spectrum. We captured 10 images of 1000 pixel $\times$ 1000 pixel in size and a resolution of 12 bits for a fixed control parameter ($\varepsilon = 0.1$) and frequency. We calculated the pattern ordering from Eq. (2) for each image. Averaging the pattern ordering from 10 images, M_p is obtained. The frequency dependence of M_p^2 for fixed $\varepsilon = 0.1$ is shown in Fig. 3.

Figure 3 shows that a transition from zero to nonzero M_p occurs at a transition frequency $f_{\mathrm{tr}} = 270$ Hz, which is close to the above-mentioned Lifshitz frequency $f_{\mathrm{L}} = 250$ Hz. Here, the small difference between f_{L} and f_{tr} was due to the small difference in ε for each experiment, that is f_{tr} is equal to f_{L}. Namely, $M_p = 0$ for the OR regime, whereas $M_p \neq 0$ for the NR regime. This means the SMT patterns in the OR and NR regimes correspond to the paramagnetic and ferromagnetic phases, respectively. The transition of the SMT patterns from the NR regime to the OR regime can be regarded as a kind of order-disorder phase transition. To interpret the above result, we use the analogy between the SMT and the conventional 2D XY model. As mentioned above, the degree of freedom of the vector fields and the spatial dimension of the systems are

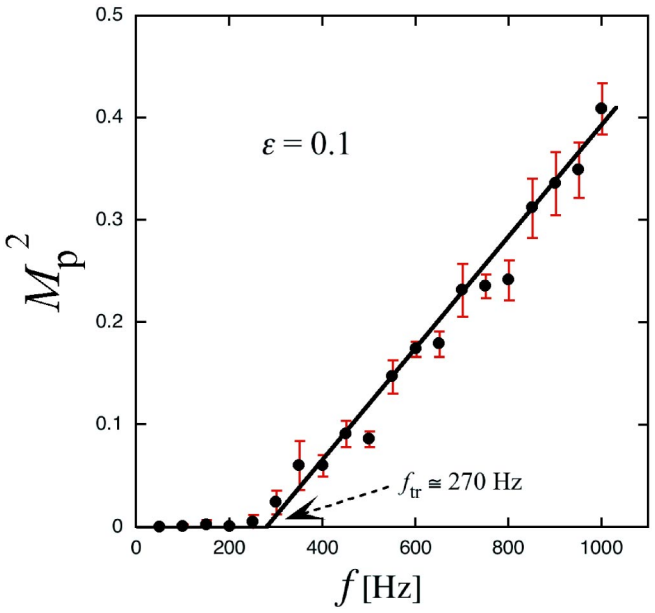

FIG. 3 (color online). Square pattern ordering M_p^2 versus frequency f for the constant control parameter ($\varepsilon = 0.1$) measured in cell II.

the same. However, the causes of the disorders are different. The disorder in the 2D XY model is caused by thermal fluctuations, whereas the disorder in the present system is caused by spatiotemporal chaos due to the nonlinear interaction between $\mathbf{C}$ and $\mathbf{q}$. Therefore, we should point out that the different mechanisms in the SMT and the 2D XY model lead to the different phenomena. Thus, in the present system, the KT transition does not occur, whereas an order-disorder phase transition is absent in the conventional 2D XY model.

To understand the role of the nonlinear interaction in both regimes, we refer to the coupled equations of the convective amplitude and the local azimuthal angle $\alpha(\mathbf{r}, t)$ of $\mathbf{C}(\mathbf{r}, t)$ [12–14]. For simplicity, we consider a stationary solution of α in the spatially uniform case. For the OR case, there is no stationary solution of α due to the existence of uncompensated torque on the $\mathbf{C}$ director. The torque generates global fluctuations in both the $\mathbf{C}$ director and the $\mathbf{q}$-wave vector through the nonlinear interaction between them. As a result, the anisotropy in the initial direction is rapidly broken, and no long-range correlation exists. On the other hand, for the NR case, there is a stationary solution $\alpha = 0$, but it is unstable. It is thought that the instability causes the $\mathbf{C}$ director to locally fluctuate around the initial direction. The local fluctuations may not break the initial anisotropy, and the wavelength of the fluctuations should be short.

Finally, the results of the present study are summarized as follows. By introducing a new order parameter, pattern ordering M_p, for the soft-mode turbulence, which is caused by the interaction between short wavelength modes and Goldstone modes, we reveal the order-disorder phase tran-

sition from the OR regime to the NR regime for increasing applied frequency. The present transition is due to the change in the symmetry for the interaction between the short wavelength and the Goldstone modes. Generally, in order to investigate the behaviors of spin systems, consideration should be given not only to the dimensions of the systems and the degrees of freedom of the spin variables, but also to the properties of the fluctuating force.

The authors would like to thank M. I. Tribelsky for engaging in many valuable discussions and H. Orihara and T. Idogaki for providing useful comments. This study was supported in part by a Grant-in-Aid for Scientific Research (B) (Grant No. 17340119) from the Ministry of Education, Culture, Sports, Science, and Technology of Japan.

*rinto@athena.ap.kyushu-u.ac.jp

[1] See, for example, A. Chatterjee and P. Sen, Phys. Rev. E **74**, 036109 (2006); G. Quirion, X. Han, M. L. Plumer, and M. Poirier, Phys. Rev. Lett. **97**, 077202 (2006).
[2] C. J. Thompson, *Classical Equilibrium Statistical Mechanics* (Clarendon, Oxford, 1988).
[3] S. Kai, K. Hayashi, and Y. Hidaka, J. Phys. Chem. **100**, 19 007 (1996).
[4] A. Hertrich, W. Decker, W. Pesch, and L. Kramer, J. Phys. II (France) **2**, 1915 (1992).
[5] H. Richter, N. Klöpper, A. Hertrich, and A. Buka, Europhys. Lett. **30**, 37 (1995).
[6] M. I. Tribelsky and K. Tsuboi, Phys. Rev. Lett. **76**, 1631 (1996).
[7] K. Tamura, R. Anugraha, R. Matsuo, Y. Hidaka, and S. Kai, J. Phys. Soc. Jpn. **75**, 063801 (2006).
[8] W. Zimmermann and L. Kramer, Phys. Rev. Lett. **55**, 402 (1985).
[9] J.-H. Huh, Y. Hidaka, and S. Kai, J. Phys. Soc. Jpn. **68**, 1567 (1999).
[10] E. Bodenschatz, W. Zimmermann, and L. Kramer, J. Phys. (Paris) **49**, 1875 (1988).
[11] Y. Hidaka, J.-H. Huh, K. Hayashi, S. Kai, and M. I. Tribelsky, Phys. Rev. E **56**, R6256 (1997).
[12] A. G. Rossberg, Ph.D. thesis, Universität Bayreuth, 1997.
[13] A. G. Rossberg and L. Kramer, Phys. Scr. **T67**, 121 (1996).
[14] A. G. Rossberg, A. Hertrich, L. Kramer, and W. Pesch, Phys. Rev. Lett. **76**, 4729 (1996).
[15] N. D. Mermin and H. Wagner, Phys. Rev. Lett. **17**, 1133 (1966).
[16] J. M. Kosterlitz and D. J. Thouless, J. Phys. C **6**, 1181 (1973).
[17] We recognize some characteristic ''black lines'' which are darker than the convective ones in the OR pattern [see Fig. 1(a)]. The black lines have been experimentally confirmed as a line defect of **C**-director. The OR and the NR regimes can be distinguished by observing the black lines, since they do not appear in the NR regime. The detailed properties of the black lines have not been investigated yet.
[18] In R-B convection system, methods for finding the azimuthal angle from patterns as well as similar definition as $\bar{D}$ for angle-angle correlation function have been done. However, there is no discussion related to phase transition. See N. Becker and G. Ahlers, J. Stat. Mech. (2006) P12002.
[19] Some types of correlation length were presented in S.-Q. Zhou and G. Ahlers, Phys. Rev. E **74**, 046212 (2006).
[20] M. Sellitto and P. C. W. Holdsworth, Fractals **11**, 73 (2003).